J Mater Sci (2010) 45:2264–2273
DOI 10.1007/s10853-009-4139-7

Thermal stability of ultrafine grains size of pure copper obtained by equal-channel angular pressing

N. Lugo · N. Llorca · J. J. Suñol · J. M. Cabrera

Received: 3 September 2009 / Accepted: 17 December 2009 / Published online: 28 January 2010

Abstract Ultrafine grain of pure copper 99.98% was produced by severe plastic deformation using the equal-channel angular pressing (ECAP) method. Copper samples were ECAPed from 1 to 8 passes following route B_C; fine grain sizes of 250 nm were developed after eight passes. Important enhancement in the mechanical strength properties was obtained. Subsequent heat treatments (HT) were carried out to evaluate the thermal stability of the grains of the ECAPed samples. Microstructure and mechanical properties were evaluated to determine the recovery and recrystallization temperatures. Differential scanning calorimetry (DSC) tests were conducted to all samples in order to determinate these temperatures. The activation energy of the recrystallization process was also determined by the DSC technique and good correlation was obtained with the microstructure and mechanical properties. An important decrease in the mechanical properties and an increasing heterogeneous grain size distribution were observed when heat treatments were performed.

N. Lugo (✉) · J. M. Cabrera
Department of Materials Science and Metallurgical Engineering ETSEIB, Polytechnic University of Catalonia, Av. Diagonal 647, 08028 Barcelona, Spain
e-mail: nayar.lugo@upc.edu

J. M. Cabrera
e-mail: jose.maria.cabrera@upc.edu

N. Llorca
Department of Materials Science and Metallurgical Engineering, University of Barcelona, C/Martí i Franqués 1-11, 08028 Barcelona, Spain
e-mail: nullorca@ub.edu

J. J. Suñol
Physics Department, University of Girona, P2, EPS, Campus Montilivi s/n, 17071 Girona, Spain
e-mail: joanjosep.sunyol@udg.es

J. M. Cabrera
CTM Technical Center, Av. Bases de Manresa 1, 08242 Manresa, Spain

Introduction

Severe plastic deformation (SPD) processes have become important in the last decade, not only because of their potential to inflict large deformations in alloys and metallic materials, but also due to their capacity in the production of ultrafine-grained microstructures within the submicrometre and nanometre ranges. Different kinds of SPD processes have been proposed, namely, high pressure torsion (HPT), accumulative roll-bonding (ARB), mechanical milling (MM), but some of them have evident limitation for industrial application because porosity and small samples are obtained. Today, one process leads the SPD field, that is, equal-channel angular pressing (ECAP) because bulk materials with homogeneous deformation can be processed [1, 2], being, therefore, very attractive for industrial applications.

In the ECAP process, a sample with cross section of a square, rectangular or circular shape can be deformed without undergoing significant changes in the dimensions, enabling significant deformations through an unlimited number of passes within a die. The ECAP die contains two channels with an equal cross section intersecting at an angle that can range typically from 90° to 135°. Dies of 90° inflict a strain ~ 1 in each pass and, after some ECAP passes, a high fraction of high-angle boundaries (>15°) is produced which contributes to a significant improvement of the mechanical properties [1–10].

Traditionally, ECAPed materials display limited ductility. This feature is also typical in materials nanostructured by other top–down techniques, such as mechanical milling and so on [11]. It has been recently suggested [12] that a possible way to increase ductility without heavy penalty on mechanical strength is the development of a duplex microstructure formed by nanometric grains sized coupled with micrometric or ultrafine grains. The latter would promote ductility while the formers would keep strength at high values. The usual way to achieve such microstructure is by a controlled heat treatment. However, scarce information can be found in the literature concerning the grain growth behaviour and thermal stability of ECAPed materials, and particularly on copper. Consequently, the aim of this research is to study the microstructural features produced by ECAP and to evaluate the thermal stability of the grains in the processed samples in order to estimate the potential resistance of the ECAPed microstructure of pure copper samples when they are subjected to subsequent heat treatments.

Experimental procedure

High-purity copper (99.98% in mass) was selected for the present study. This copper was supplied in a cold-drawn state. An annealing treatment was performed to the as-received material (600 °C for 2 h), giving a grain size of ~60 μm and a hardness of 65 HV. Bars of the as-received material were then machined to obtain cylindrical samples with 10 mm in diameter and 60 mm in length for ECAP processing.

ECAP was conducted at room temperature using a die with a channel angle of 90° and an angle of 20° for the outer arc of curvature. Samples were pressed from 1 to 8 passes through route B_C, i.e. the sample was rotated along the longitudinal axis by 90° [5, 6]. As already mentioned, the total equivalent strain introduced in this ECAP process was ~1 in each pass reaching a strain ~8 at the 8th pass [13]. Samples for heat treatments were obtained from all ECAPed specimens. For this purpose, transverse sections (perpendicular to the extruding direction ED) of 2 mm thick were sliced from the cylindrical pressed specimens (Fig. 1). The material was annealed at various temperatures between 100 and 600 °C for 30 min in a tubular furnace under an Ar inert atmosphere. After solution treatment, samples were quenched in water to retain the microstructure.

Microstructures were observed through optical microscopy with an Olympus GX51. Samples were prepared following conventional metallographic preparation, grinding, electro-polishing and finally they were electro-etched

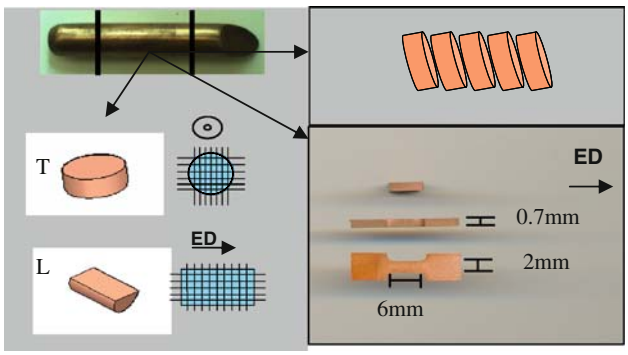

Fig. 1 Zones of sample extraction for: heat treatments (*upper right*), microhardness measurements of the transversal section (T) and longitudinal section (L) (*left*) and tensile tests (*lower right*). The extrusion direction (ED) is indicated for the testing samples

in a solution of 3% nitric acid in methanol. Transmission electron microscopy (TEM) was carried out in a High Resolution TEM CM-30 Phillips (300 kV). TEM samples were prepared by accurate grinding and concave polishing followed by a Precision Ion Polishing System (Model 691 PIPS, GATAN Inc.). TEM samples were also used to evaluate the dislocation density after each pass.

Mechanical property data at room temperature was obtained from all ECAPed specimens (processed and not heat treated and processed + heat treatment) either from microhardness (see Fig. 1 left) or microtensile tests (see Fig. 1 lower right). The microhardness tests were carried out using an AKASHI hardness-testing machine with an applied load of 50 g for 15 s. Measurements were taken along a series of well-defined traverses on each polished surface as depicted in Fig. 1, screening both the cross section perpendicular to the extrusion direction (ED) and the longitudinal section parallel to the extrusion direction as well. The individual measurements were then plotted comparing processed and processed plus heated samples. The tensile tests were performed on 0.7 mm thick specimens whose gauge dimensions were 2 mm width and 6 mm length extracted from the billets in the extrusion direction (see Fig. 1). They were deformed at an initial strain rate of 3.3×10^{-3} s^{-1} at room temperature using an INSTRON testing machine.

In order to determine calorimetric information, differential scanning calorimeter (DSC) analysis was carried out using a Perkin-Elmer DSC-7 system. Discs of 3 mm diameter and 120 μm thickness were previously cleaned in a 3% HNO_3 solution to eliminate oxides and contamination and were then placed in close contact with an aluminium pan, which was in turn placed into a platinum sample holder in the Calorimeter. High purity Ar gas was introduced to protect the sample from oxidation during thermal scanning.

Experimental results

Microstructure

ECAP specimens

The microstructure of the unprocessed annealed Cu shown in Fig. 2 consists of equiaxed grains with an average size of 60 μm and some twinning.

The microstructures of the ECAP samples processed from 1 to 8 passes through the die are illustrated in Fig. 3. It is evident the significant elongation of the grains since the first pass as well as the refinement induced by the process. The severe deformation introduced in subsequent passes makes difficult to analyze the microstructure solely by optical microscopy. Even with this difficulty, there is one fact that can clearly be seen especially for the first pass through the ECAP die, which is a sort of rearrangement in grouped elongated grains at an angle close to 45°. For the second pass, grains can still be seen, however, multiple directionality is detected, and grains seem to be grouped following them. After the third pass, the microstructure becomes highly refined and could not be resolved by OM. Additionally, the typical annealing twins tend to disappear or cannot be observed due to the severe strain imposed.

A detailed microstructure examination by TEM has confirmed the presence of highly deformed microstructures after the second ECAP pass, being more evident in subsequent passes (see Fig. 4). These micrographs also show a significant decrease in the grain size with regard to the undeformed material but also along the ECAP process. This grain refinement is produced by the heavy deformation introduced in each pass. A very high dislocation density is introduced in the early stages of the ECAP process. Dislocations cells structures, as a result of the highly mobile dislocations, can be seen in this step of the process. The microstructure becomes more elongated in the second pass through the die, these elongated subgrains transform, in the third pass, to more equiaxed subgrains with a significant quantity of mobile dislocations inside increasing their grain misorientation. With the following passes they become elongated again until the seventh pass that shows a very equiaxed and refined microstructure with grain sizes ranging between 200 and 500 nm.

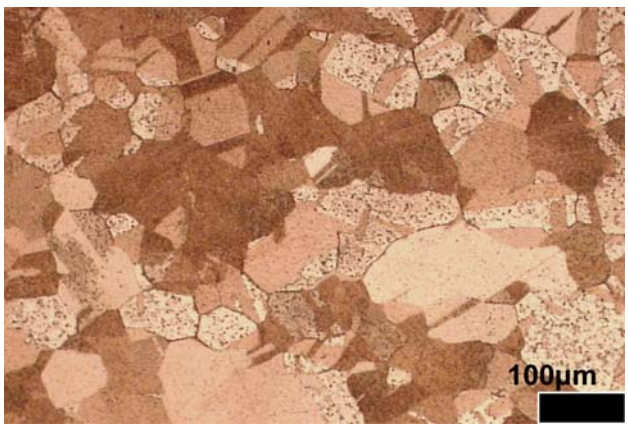

Fig. 2 Microstructure of unprocessed Cu annealed at 600 °C for 2 h (OM)

ECAP + annealing specimens

After heat treatments, TEM observations were also carried out on sliced discs on the transverse direction (Fig. 1 upper right). Significant changes in grain size and aspect ratio were observed as the treatment temperature raises, except for the samples annealed at 100 °C (see Fig. 5) where the microstructure is similar to the sample ECAP processed at room temperature independently of the pass number given to the sample.

At the lowest temperature of annealing a rearrangement of the subgrain and defect (dislocation) structure can be seen, indicating that some recovery of the microstructure is taking place. This is clearly observed when comparing, for example, samples with 1 and 2 passes after being heat treated (top micrographs in Fig. 5) for which fine well defined 'boundaries' were developed for the latter.

An important increase in grain size was observed after heating at temperatures higher than 300 °C irrespective of the number of passes given to the specimen. Paradoxically, grain growth was moderate in more severely deformed samples and for specimen processed with 4 and 8 passes treated at 200 and 300 °C showed lower growth than that showed by the specimen ECAPed once. However, treatments at temperatures higher or equal to 400 °C, produced grains growing rapidly but heterogeneously, especially for passes 1 and 4 for which microstructure with bimodal grain size was clearly observed. Figure 6 shows the microstructures performed by the annealing treatments at 300 and 400 °C after several strain conditions for the ECAPed samples.

The coexistence of small and large grain sizes is probably originated by a heterogeneous strained material. Under these conditions, highly deformed grains will reach the recrystallization condition before than other grains less strained and should start to recrystallize before them, promoting a heterogeneous grain size leading to bimodal distribution. Heat treatments at higher temperatures (>500 °C) favour the growth of grains refined after ECAP. As stated by Zhou et al. [14], non-uniform microstructure was formed via recovery and recrystallization during annealing of nanocrystalline Al–Mg powders with a non-homogenous structure produced by cryo-milling,

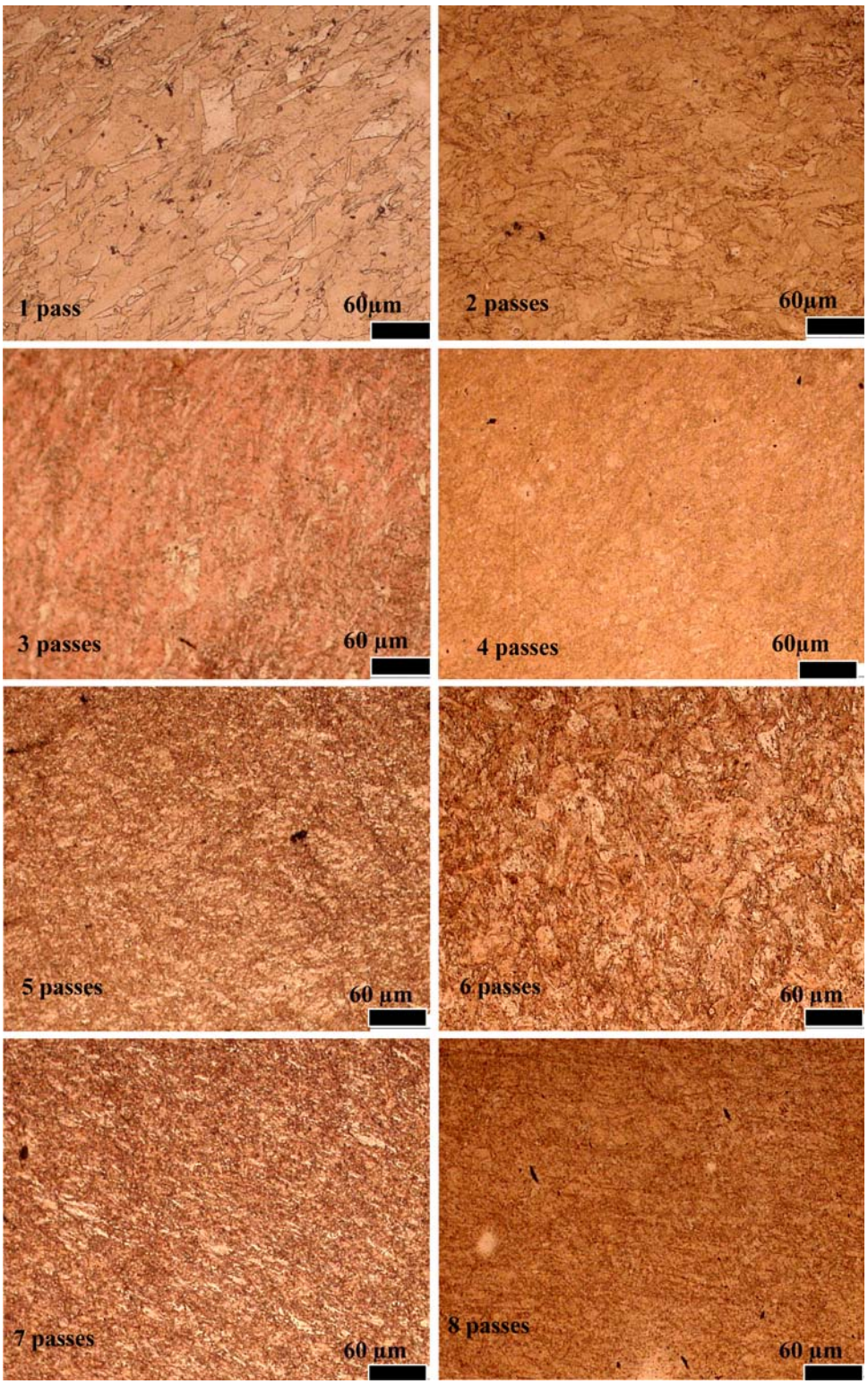

Fig. 3 Microstructure of Cu after ECAP from 1 to 8 passes (OM) micrographs show the longitudinal section of the billet parallel to the ED

for which large-sized grains were growing into the matrix of nanometre-sized grains. As suggested in their paper, differences of defect structures may affect subgrain coarsening during the recovery process. In the present study, the differences in the microstructure of the severely deformed specimens are related to the non-uniform strained material, and hence, to the locally stored energy. This would drive to different recovery and recrystallization paths in the material that would produce the observed final bimodal microstructure.

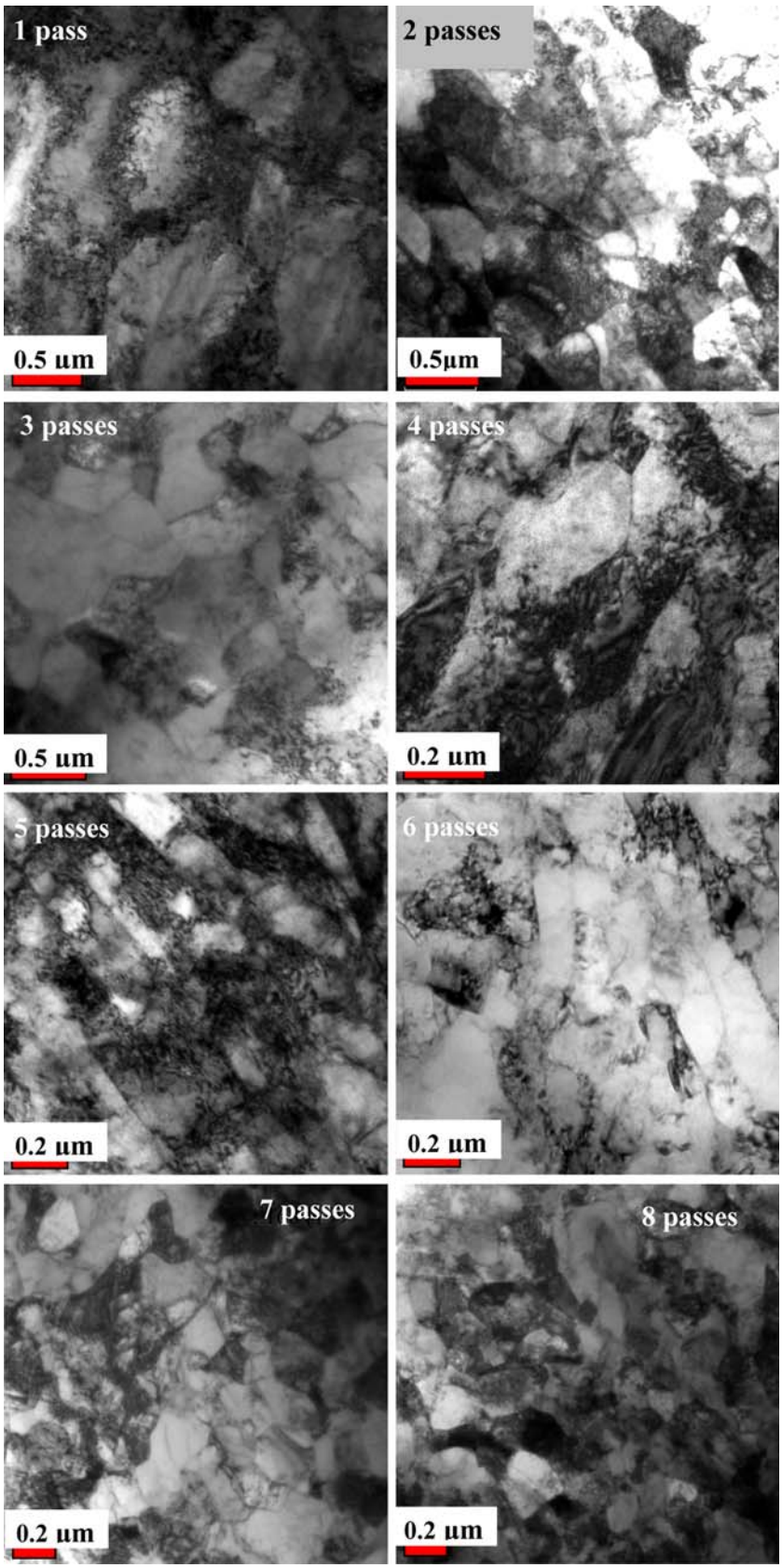

Fig. 4 TEM micrographs of a non-heat treated ECAP samples

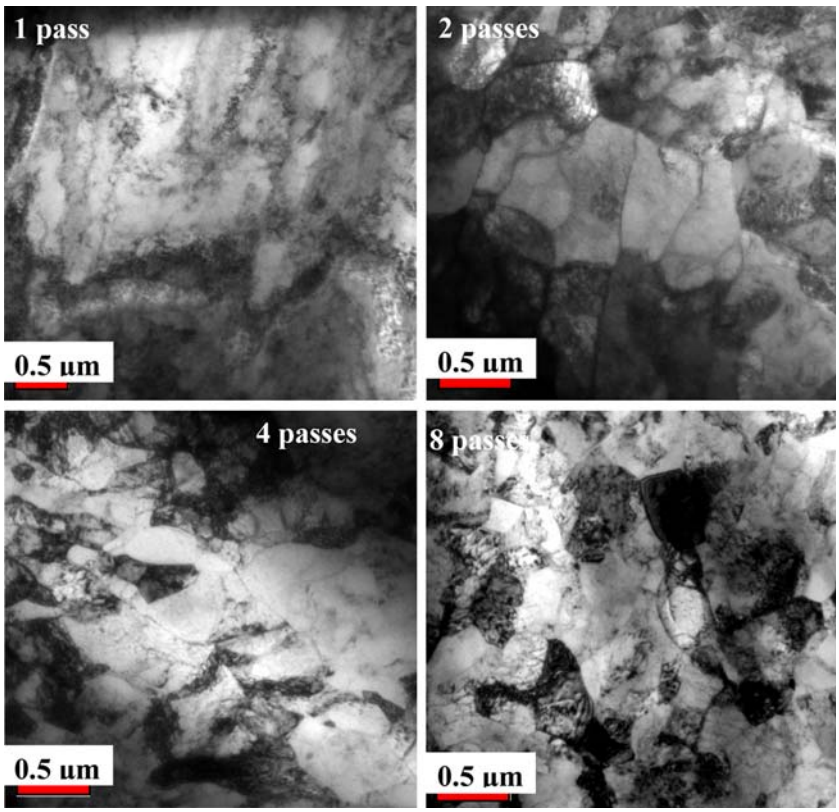

Fig. 5 TEM micrograph for cross section ECAP samples after heat treatment at 100 °C

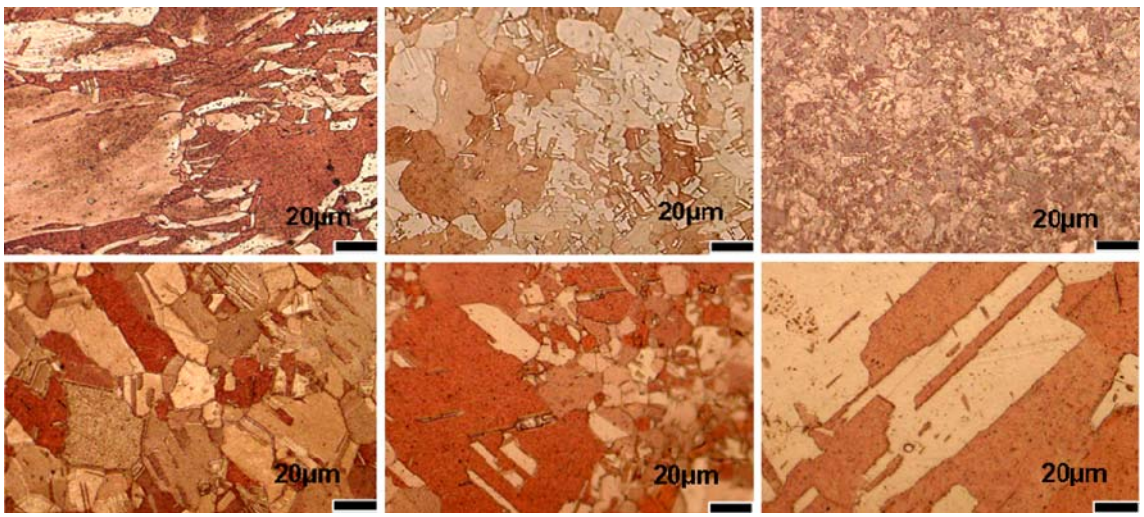

Fig. 6 Microstructures of annealed 1 pass (*left*), 4 passes (*centre*) and 8 passes (*right*) samples at 300 °C (*top range*) and 400 °C (*bottom range*)

Grain size determination of the ECAPed samples was carried out through several micrographs taken from optical and transmission electron microscopes. The grain size versus ECAP pass dependence is shown in Fig. 7. It can be noticed that grain size ranges between 150 and 300 nm in the ECAP samples as well as in the ECAP + annealing at 100 °C samples. According to the representation of the two latter conditions, grain size distribution is rather similar for both and no evidence of recrystallization seems to be involved.

A similar analysis was applied to the ECAP samples after heat treatment (see Fig. 7). It is worth noting that the recrystallized grain size decreases at increasing ECAP pass. After 200 °C, it is clear that recrystallization and grain growth process are present in all samples. Most grains contain annealing twins, providing evidence that

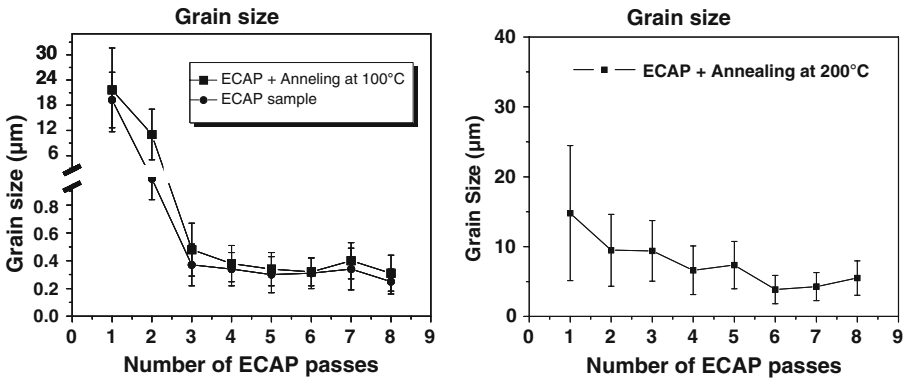

Fig. 7 Dependence of the grain size with the number of ECAP passes for severely deformed samples and samples ECAP processed + annealing at 100 °C and 200 °C (*right*) during 30 min

recrystallization has occurred. It is obvious that this is due to the progress of static recrystallization promoted by the large strain introduced in the material and the temperatures attained during the heat treatment. One must keep in mind that commercially pure copper can recrystallize at temperatures as low as 200 °C [15] and, taking into account the high strain introduced in the material, the temperature was lowered with the number of passes the samples were processed through the die.

Dislocation density

It is well known that conventional coarse-grained metals can be softened by annealing and strengthened by cold working. Annealing reduces the dislocation density in materials while cold work increases it. Table 1 reports the results of the TEM dislocation density values obtained using Ham methodology [16]. As can be seen, the first pass introduced the larger amount of dislocations. Subsequent ECAP passes introduces more dislocations, but in a more gradual way than in the first pass. This increment is produced due to high deformation imposed in each pass. However, after the fifth pass a clear decrease in the dislocation density is appreciated. The dislocation density reduction after the fifth pass through the ECAP die is due to the rearrangement of mobile dislocations by recovery which produces in turns ultrafine grain structure as illustrated in Fig. 5.

Table 1 Dislocation density values for ECAP samples and dislocation density differences between passes

Sample	Dislocation density ρ $(m^{-2}) \times 10^{+14}$	$\Delta\rho$ $(m^{-2}) \times 10^{+14}$
Cu unprocessed	0.29 ± 0.07	–
ECAP-1 pass	3.45 ± 0.19	3.16
ECAP-2 passes	4.02 ± 1.99	0.57
ECAP-3 passes	4.89 ± 0.27	0.87
ECAP-4 passes	6.89 ± 0.18	2.00
ECAP-5 passes	8.12 ± 0.49	1.23
ECAP-6 passes	7.36 ± 0.13	−0.76
ECAP-7 passes	6.32 ± 0.41	−1.04
ECAP-8 passes	4.09 ± 0.41	−2.23

Mechanical behaviour

Microhardness determination

As already mentioned, Vickers microhardness measurements were carried out along the longitudinal and transversal sections as illustrated in Fig. 1. Longitudinal hardness measurements were, for all the samples, more homogeneous than transversal sections measurements. As stated in reference [2], the initial four passes introduced anisotropy in the samples as also can be observed in the microstructure, whereas from the fifth pass the samples behaved showing lower heterogeneities in hardness values.

After one ECAP pass, a significant increase in the hardness over the corresponding annealed state is observed as plotted in Fig. 8. A more gradual increment is noticed in subsequent passes. The microhardness behaviour for samples annealed at 100 °C is very different that the obtained for samples annealed at 200 °C as can be seen in the

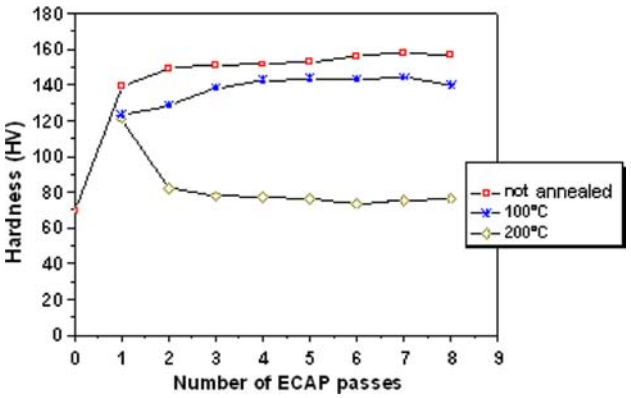

Fig. 8 Microhardness values for ECAP sample at room temperature (*open square*) and after heat treatments

representation. It seems that for ECAP + annealing at 100 °C samples, the essential softening process must be recovery. The same applies for ECAP + annealing at 200 °C samples after the first pass. However, the subsequent passes at the same temperature produced static recrystallization.

Microtensile tests

Additional evaluation of the mechanical properties of the ECAP-processed samples was undertaken by microtensile tests. Yield strength and ultimate tensile strength obtained (listed in Table 2) are in agreement with the hardness values reported in the previous paragraph. Flow curves are plotted in Fig. 9. Only tensile tests were carried out for three different conditions—unprocessed, processed and annealed at 100 °C and processed and annealed at 200 °C, because after this temperature hardness values reported a low value and very similar for every temperature. One can notice that the largest strength was obtained in the sample deformed by ECAP at room temperature, followed by samples heated at 100 °C, and finally those treated at 200 °C. In terms of ductility, in the two-first conditions (room temperature and 100 °C) samples show similar values ($\varepsilon \sim 0.3$) which is almost half of the annealed material. However, the elongation to failure can give a false impression of high ductility in samples with very short gauge length due to large post-necking strain [17]. Instead, uniform elongation can be used as a measure of ductility. Another alternative is the evaluation of the transversal fractured area (%RA in Table 2) because most deformation after necking is located in this area. High %RA values were found in all the samples. It is worth noting that, beside the fact that a significant improvement in material resistance is produced in ECAP samples, no heavy penalization on ductility is found. However, a strong decrease in strength is observed after treatment at 200 °C, indicating that recrystallization must be occurring; in full agreement with hardness values (Fig. 7).

Table 2 Mechanical properties after tensile tests

Sample	ECAP			ECAP + 100 °C			ECAP + 200 °C		
	YS	UTS	RA	YS	UTS	RA	YS	UTS	RA
Starting material	90	249	94	90	249	94	90	249	94
1 pass	363	377	85	318	361	85	276	298	85
2 passes	362	392	88	355	361	86	105	244	91
3 passes	377	407	87	319	356	86	121	255	93
4 passes	412	435	88	319	366	87	60	262	94
5 passes	409	444	87	344	374	88	94	258	93
6 passes	438	457	89	342	385	85	75	260	94
7 passes	447	470	89	352	395	88	73	264	94
8 passes	472	488	92	381	420	90	58	270	93

YS yield strength in MPa, *UTS* ultimate tensile strength in MPa, *RA* average reduction in area in %

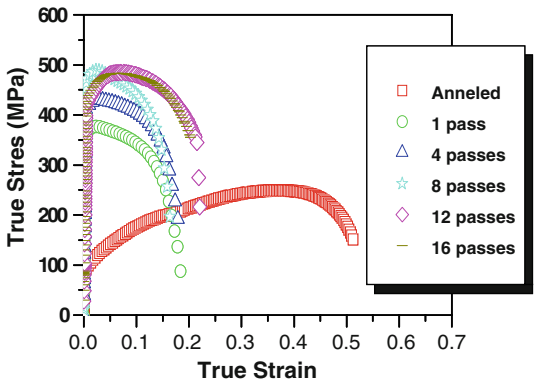

Fig. 9 Microtensile test representation for ECAPed and starting material samples

Thermal behaviour of ECAP samples

DSC curves of ECAP samples are shown in Fig. 10. The curves are obtained under a heating rate of 10 °C min^{-1} and evidence of one exothermic peak is found. Some authors have suggested that the DSC peaks can be associated initially to static recrystallization process [17]. It is

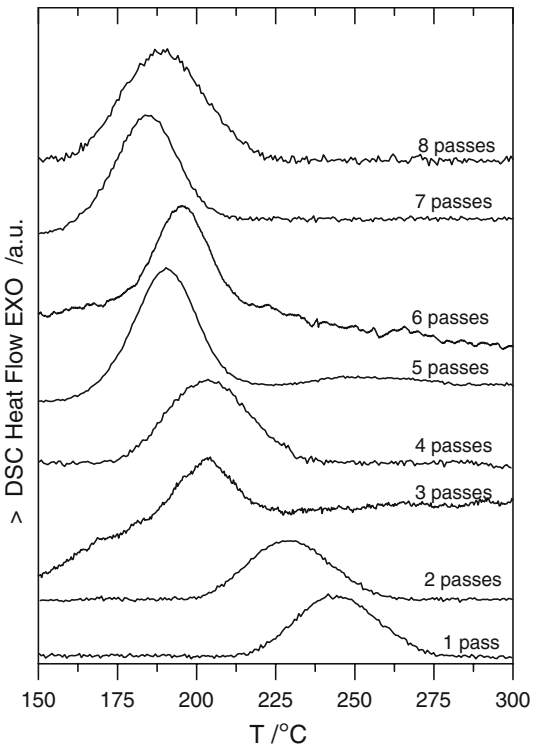

Fig. 10 DSC graphs for all ECAP samples

possible to obtain several peaks, but in the present study, DSC tests produced only one peak. From the microstructure characterization, this peak can be associated to recovery especially for the initial passes.

The values of the enthalpies associated to the peaks are reported in Table 3. One can notice that enthalpy is initially constant and relatively low, 0.4 J/g (25.40 J/mol), increases continuously until reaching a maximum energy of 1.39 J/g (88.26 J/mol) at five passes and then decreases to a value of 0.8 J/g (50.80 J/mol) higher than at the first pass.

The dependence of the initial temperature for the recovery and recrystallization (T_o) and the peak temperature (T_p) on the plastic deformation (i.e. on the ECAP passes) is illustrated in Fig. 11. When the number of ECAP passes increases, the onset temperature and the peak temperature also decrease. Although this is an expected result, no evidence of a clear saturation temperature with the amount of deformation is observed. A heat treatment around 170 °C would probably promote lower diminution of strength while increasing the ductility.

Table 3 Enthalpy (ΔH), onset temperature (T_o) and peak temperature (T_p) obtained from the DSC diagrams

Sample	ΔH (J g^{-1}) (±5%)	T_o (°C) (±1 °C)	T_p (°C) (±1 °C)
1 pass	0.40	218	244
2 passes	0.41	204	229
3 passes	0.48	184	205
4 passes	0.61	178	203
5 passes	1.39	165	191
6 passes	0.81	180	196
7 passes	0.68	169	183
8 passes	0.88	170	191

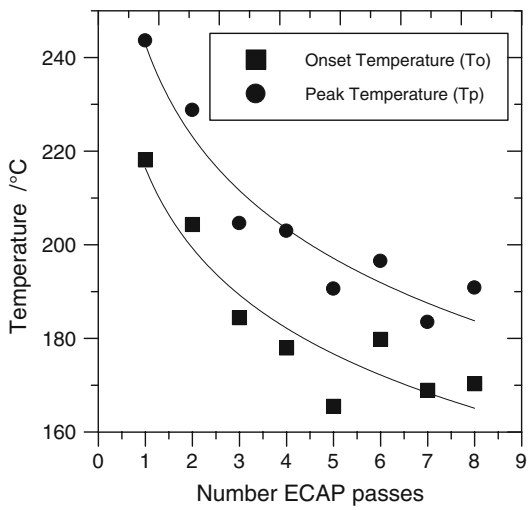

Fig. 11 Dependence of the onset temperature (T_o) and the peak temperature (T_p) on the number of ECAP passes

In order to evaluate the activation energy for the ECAP process, DSC analyzes were carried out at three different heating rates: 10, 20 and 40 °C min^{-1} but only to samples of 1, 5 and 8 passes. The Kissinger analysis of nucleation-and-growth [18, 19] was used to calculate the activation energy according to the following equation:

$$\mathrm{Ln}\left(\frac{\beta}{T_p^2}\right) = -\frac{Q}{K_b}\frac{1}{T_p} + k_0 \quad (1)$$

where β is the DSC heating rate, T_p is the peak temperature, Q is the activation energy, K_b is the Boltzmann constant and k_0 is a constant. According to the Kissinger graph of Fig. 12, equal values are observed for the 1st, 5th and 8th passes with respect to the activation energy (see Table 4). In consequence no important influence in the activation energy is introduced at increasing deformation, i.e. number of ECAP passes. These results confirm that recrystallization has already occurred in samples heated at 200 °C and, in agreement with previous results; the improvement in mechanical properties is lost.

Another observation is that the activation energy is close to 120 kJ/mol for all ECAP samples analyzed. This value is of the similar magnitude to the activation energy showed by other SPD processes for copper: for example, recrystallization-and-growth reported for copper severely deformed under the high pressure torsion (HPT) process

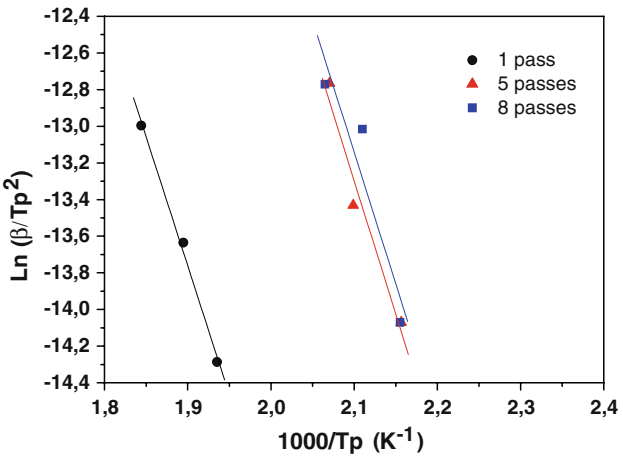

Fig. 12 Kissinger graph for all ECAP 1, 5 and 8 passes

Table 4 Activation energy associated to recovery and recrystallization in ECAP process

Sample	Activation energy (kJ/mol)	Correlation coefficient, r^2
Cu-1 pass	117 ± 2	0.99
Cu-5 passes	121 ± 5	0.95
Cu-8 passes	119 ± 11	0.88

(94.56 kJ/mol) [20], grain growth of cold compacted nanocrystalline copper (100.39 kJ/mol) [21] and nano crystalline copper prepared by inert gas consolidation (82.98 kJ/mol) [22, 23] all of them obtained by the same Kissinger analysis. The differences are in accordance with the statements suggested by Suwas et al. [24] for which the different processing routes in ECAP processes have significant effect on the amount of stored energy which is likely to affect the grain refinement process. There are more complex models to perform the kinetic analysis, as the isoconversional methods analyzed in the ICTAC kinetics project [25]. Nevertheless, the correlation coefficient allows us to state that Kissinger methods provides an acceptable value of the activation energy and it is the method used in the references here introduced to compare the activation energy values.

Thermally activated energy, which varies linearly with static recovered strain, was calculated from static recovery experiments of pure copper initially deformed by strain-rate-controlled tensile tests by Kuo and Lin [26]. By the evidence of dislocation morphology, the authors found that the activation energy at the initial static recovery was 48 kJ mol^{-1}, which is the energy for dislocation annihilation by glide or cross-slip. Once dislocation annihilation processes are exhausted, more energy is required for subgrains to form and then grow. The recovered strain is slowed down and eventually saturated.

Conclusions

1. The processes of SPD ECAP are effective for the production of ultrafine-grained microstructures of commercially pure copper. A significant increase in the mechanical strength has been observed after subjecting the material to ECAP.
2. The thermal stability of commercially pure Copper processed by ECAP (Route B_C) was investigated. Calorimetric measurements revealed only one exothermic peak when annealing samples with different number of ECAP passes. The DSC peak was spread and was associated to recovery and recrystallization processes although the grain size showed by the samples annealed at 100 °C was similar to the deformed samples. The onset of the recrystallization process is close to 200 °C and depends on the amount of deformation stored, the larger the strain the lower the recrystallization temperature. The activation energy for this process is $\sim$120 kJ/mol.
3. Annealed samples exhibited non-uniform grain morphologies and size distribution, which derived from differences in the energy stored in the severely deformed material. This is clearly seen for temperatures higher than 200 °C.
4. With the recrystallization process the increase in the mechanical strength in ECAP processes disappears due to the fast recrystallization and grain growth phenomena.

Acknowledgements Thanks are given to the Ministry of Science and Technology of Spain for supporting the project DPI2005-09324-C02-01. NL thanks the scholarship (BES-2003-2754) granted by the Ministry of Science and Technology of Spain.

References

1. Segal VM, Reznikov VI, Drobyshevskiy AE, Kopylov VI (1981) Russ Metall 99
2. Lugo N, Llorca N, Cabrera JM, Horita Z (2008) Mater Sci Eng A 477:366
3. Valiev RZ, Krasilinikov NA, Tsenev NK (1991) Mater Sci Eng A 137:35
4. Nakashima K, Horita Z, Nemoto M, Langdon TG (1998) Acta Mater 46:1589
5. Iwahashi Y, Horita Z, Nemoto M, Langdon TG (1998) Acta Mater 46:3317
6. Furukawa M, Horita Z, Nemoto N, Langdon TG (2001) J Mater Sci 36:2835. doi:10.1023/A:1017932417043
7. Ma X, Lapovok R, Gu C, Molotnikov A, Estrin Y, Perelona EV, Davies CHJ, Hodgson PD (2009) J Mater Sci 44:3807. doi: 10.1007/s10853-009-3515-7
8. Kumar P, Xu C, Langdon TG (2009) J Mater Sci 44:3913. doi: 10.1007/s10853-009-3535-3
9. Zhang Y, Wang JT, Cheng C (2008) J Mater Sci 43:7326. doi: 10.1007/s10853-008-2903-8
10. Wang YB, Ho JC, Cao Y, Li HQ, Zhao YH, Lavernia EJ, Ringer SP, Zhu YT (2009) Appl Phys Lett 94:91911
11. Jia D, Ramesh KT, Ma E (2003) Acta Mater 51:3495
12. Srinivasarao B, Oh-ishi K, Ohkubo T, Hono K (2009) Acta Mater 57:3277
13. Iwahashi Y, Wang J, Horita Z, Nemoto M, Langdon TG (1996) Scripta Mater 35:143
14. Zhou F, Liao XZ, Zhu YT, Dalleck S, Lavernia EJ (2003) Acta Mater 51:2777
15. Krüger P, Woldt E (1992) Acta Metall Mater 40:2933
16. Ham RK (1961) Philos Mag 6:1183
17. Zhao Y, Liao X, Cheng S, Ma E, Zhu YT (2006) Adv Mater 18:2280
18. Kissinger HE (1957) Anal Chem 29:1702
19. Chen LC, Spaepen F (1991) J Appl Phys 69:679
20. Jiang H, Zhu YT, Butt PDP, Alexandrov IV, Lowe TC (2000) Mater Sci Eng A 290:128
21. Huang YK, Menovsky AA, de Boer FR (1993) Nanostruct Mater 2:587
22. Gunther G, Kumpmann A, Kunze HD (1992) Scripta Metall Mater 27:833
23. Kumpmann A, Gunther G, Kunze HD (1993) Mater Sci Eng A 168:165
24. Suwas S, Eberhardt A, Toth LS, Fundenberger JJ, Grosdidier T (2004) Mater Sci Forum 467–470:1325
25. Vyazovkin S (2000) Thermochim Acta 355:15
26. Kuo C, Lin C (2003) Scripta Mater 57:667